JOURNAL OF CATALYSIS 83, 131–140 (1983)

Deuterium Isotope Effects for Hydrocarbon Reactions Catalyzed over Platinum Single Crystal Surfaces

S. M. DAVIS,[1] W. D. GILLESPIE,[2] AND G. A. SOMORJAI

Materials and Molecular Research Division, Lawrence Berkeley Laboratory, and Department of Chemistry, University of California, Berkeley, California 94720

Received December 21, 1982; revised April 29, 1983

The initial rates of isobutane, neopentane, cyclohexane, *n*-hexane, and *n*-heptane skeletal rearrangement reactions catalyzed in the presence of deuterium gas over the flat(111), stepped(13,1,1), and kinked(10,8,7) platinum single crystal surfaces were measured at atmospheric pressures and 520–640 K. Inverse isotope effects [$(R_D/R_H) = 1.3–3.3$] were detected for a variety of hydrogenolysis, isomerization, and C_5 cyclization reactions. The inverse isotope effects that appear to arise from a combination of kinetic and thermodynamic isotope effects displayed magnitudes that were not dependent on the platinum surface structure.

INTRODUCTION

Important information about the elementary steps of catalyzed surface reactions involving hydrogen containing molecules can often be derived from studies of deuterium isotope effects. As discussed by Ozaki (*1*), two major types of deuterium isotope effects can be distinguished: kinetic and thermodynamic. A kinetic isotope effect on the rate of reaction arises when rate constants differ for reactions carried out in hydrogen and deuterium or with deuterated reactants. Because deuterium makes larger contributions to translational and rotational partition functions than hydrogen, and because X–D bonds (X=C, N, O, etc.) possess lower zero point energies than X–H bonds, rate constants for deuterium addition and X–D scission are generally smaller than those for H addition and X–H scission, respectively ($k_H > k_D$). Alcohol dehydration (*2*) and olefin hydrogenation (*3*) are reactions which display kinetic isotope effects with magnitudes in the range $R_H/R_D = 1.5–4.5$.

By contrast, thermodynamic isotope effects originate from a change in the equilibrium surface concentration of a reaction intermediate. Detailed interpretation of these effects can be difficult because the thermodynamic effect usually appears in combination with a kinetic isotope effect, i.e., $R_H/R_D \simeq k_H\theta_{XH}/k_D\theta_{XD}$ (*4*). However, "inverse" deuterium isotope effects with magnitudes $R_D/R_H = 1.4–3.5$ have been clearly established for several types of reactions including CO hydrogenation (deuteration) over silica supported ruthenium (*5*) and ammonia synthesis over unpromoted iron (*6*). For these reactions, the thermodynamic isotope effects appear to be larger than the kinetic isotope effects and, therefore, the reaction rates are increased in the presence of deuterium.

Recent studies in our laboratory (*7*) demonstrated that *n*-hexane, *n*-heptane, and isobutane deuterium exchange reactions catalyzed near atmospheric pressure over platinum single crystal surfaces take place very rapidly as compared with the initial rates of hydrocarbon conversion reactions to form hydrogenolysis, isomerization, dehydrogenation, and dehydrocyclization products. Provided that the reaction intermediates leading to hydrocarbon conversion in the presence of deuterium are partially deuterated, thermodynamic isotope effects should exist for the skeletal rear-

[1] Permanent Address: Exxon Research and Development Laboratory, P.O. Box 2226, Baton Rouge, La. 70821.

[2] Permanent Address: Shell Development Company, P.O. Box 1380, Houston, Tex. 77001.

0021-9517/83 $3.00

rangement reactions. Inverse deuterium isotope effects were, in fact, detected for a wide variety of reactions, and these isotope effects form the subject of this report.

It was discovered that the rates of alkane hydrogenolysis, isomerization, and cyclization reactions catalyzed in excess deuterium at 520–640 K are about 1.4–3.0 times higher than the rates of the same reactions in hydrogen under identical experimental conditions. The magnitude of these isotope effects depends little if at all on platinum surface structure and appears to decrease slightly with increasing temperature. A change in selectivity results when parallel reactions display isotope effects with different magnitudes. To the best of our knowledge, deuterium isotope effects for metal catalyzed hydrocarbon skeletal rearrangement reactions have not been previously considered.

EXPERIMENTAL

The apparatus for combined surface analysis (LEED and AES) and catalysis studies, experimental procedures, and most of the materials used for the isotope effect studies were described in detail in recent papers (*7, 8*). It should be recalled that the sample isolation cell and external recirculation system operates in the 10^{-1}–10 atm pressure range as a well-mixed microbatch reactor with on-line product analysis by gas chromatography. All reagents were of the highest obtainable research purity: isobutane and neopentane (Matheson, >99.98 mole%), cyclohexane, *n*-hexane, and *n*-heptane (Phillips, >99.996 mole%), hydrogen and deuterium (LBL–Matheson, >99.99 mole%). In addition to the flat, hexagonal (111) platinum surface, stepped (13,1,1) and kinked (10,8,7) platinum single crystal surfaces were used in the reaction rate studies. The Pt(13,1,1) surface has terraces of square (100) orientation that average seven atoms in width which are separated by atomic steps, one atom in height, of (111) orientation. The (10,8,7) surface has (111) terraces that average five atoms in width that are displaced by atomic steps of (310) orientation. The dependence of the reaction rates on pressure, temperature, and surface structure is described elsewhere (*7, 8*).

Isothermal retention times measured on a 0.19% picric acid on 80/100 carbopack column were used to estimate the average deuterium content of the reaction products that were produced in the hydrocarbon conversion reactions. In the presence of deuterium, the gas chromatograms were always shifted 4–6% toward shorter retention times as compared to the retention times that were measured in hydrogen, e.g. $t_R^{n\text{-}C_6H_{14}} = 8.9$ min, $t_R^{n\text{-}C_6D_{14}} = 8.45$ min, $t_R^{rxn} =$ 8.95 and 8.45 min; $t_R^{C_6H_6} = 9.6$ min, $t_R^{C_6D_6} =$ 9.3 min, $t_R^{rxn} = 9.35$–9.42 min. These shifts indicate that the reaction products were always extensively deuterated, most probably perdeuterated (*9*). Exchange distributions for the reaction products appeared to be narrow because the chromatograms for each product were always sharp, never broadened detectably, and always shifted by the same time independent of reaction temperature and pressure.

RESULTS AND DISCUSSION

Scope of the Isotope Effect

Initial reaction rates in deuterium and inverse deuterium isotope effects measured for a variety of hydrocarbon reactions catalyzed at 573 K over the flat (111), stepped (13,1,1), and kinked (10,8,7) platinum surfaces are summarized in Table 1. Magnitudes of the deuterium isotope effects were estimated graphically from the initial slopes of product accumulation curves determined as a function of reaction time in the presence of hydrogen and in deuterium. Example product accumulation curves for *n*-hexane isomerization to 2-methylpentane and cyclization to methylcyclopentane over Pt(111) are shown in Fig. 1. Hydrogenolysis reactions of isobutane, neopentane, *n*-hexane, cyclohexane, and *n*-heptane all displayed inverse isotope effects with magni-

TABLE 1

Initial Reaction Rates in Deuterium and Deuterium Isotope Effects Measured for Hydrocarbon Reactions Catalyzed at 573 K over the Flat (111), Stepped (13,1,1), and Kinked (10,8,7) Platinum Single Crystal Surfaces[a]

Reactant	Reaction	Initial turnover frequency (molecules/Pt atom sec) (±15%)			Inverse isotope effect (R_D/R_H) (±30%)		
		Pt(111)	Pt(10,8,7)	Pt(13,1,1)	Pt(111)	Pt(10,8,7)	Pt(13,1,1)
Isobutane	Hydrogenolysis	0.0064	0.019	—	1.8	1.4	—
	Isomerization	0.053	0.075	—	1.7	1.3	—
Neopentane	Hydrogenolysis	—	0.0047[b]	0.048	—	1.7[b]	2.0
	Isomerization	—	0.020[b]	0.40	—	1.5[b]	2.0
Cyclohexane	Hydrogenolysis	0.005[c]	—	—	2.0[c]	—	—
	Dehydrogenation	9.6[c]	—	—	1.2[c]	—	—
n-Hexane	Hydrogenolysis	0.016	0.0089	0.013	1.8	1.4	1.9
	Isomerization	0.014	—	0.0090	1.7	—	2.1
	Cyclization	0.014	—	0.018	1.7	—	1.9
	Aromatization	0.0047	0.0042	—	0.9	0.8	—
n-Heptane	Hydrogenolysis	0.021[d]	—	—	1.6[d]	—	—
	Aromatization	0.0074[d]	—	—	0.8[d]	—	—

[a] Reaction conditions, D_2/HC = 10, P_{tot} = 220 Torr, 573 K.
[b] At 543 K.
[c] D_2/HC = 6.7, P_{tot} = 115 Torr.
[d] D_2/HC = 32, P_{tot} = 495 Torr.

tudes in the range R_D/R_H = 1.3–1.8. The hydrogenolysis product distributions were unchanged. For isomerization reactions, the isotope effects were in the range R_D/R_H = 1.2–3.2. Isomerization of *n*-hexane to 2-methylpentane displayed the largest isotope effect (R_D/R_H = 2.5–3.2), whereas *n*-hexane isomerization to 3-methylpentane displayed a smaller effect (R_D/R_H = 1.2–1.5). Isomerization and hydrogenolysis of isobutane and neopentane displayed isotope effects with equal magnitudes on all surfaces investigated. Cyclohexane dehydrogenation to benzene over Pt(111) appeared to exhibit a small inverse isotope effect ($R_D/R_H \approx 1.2$), whereas aromatization of *n*-hexane and *n*-heptane over Pt(111) and Pt(10,8,7) displayed unique behavior characterized by a small kinetic isotope effect ($R_D/R_H \lesssim 1$).

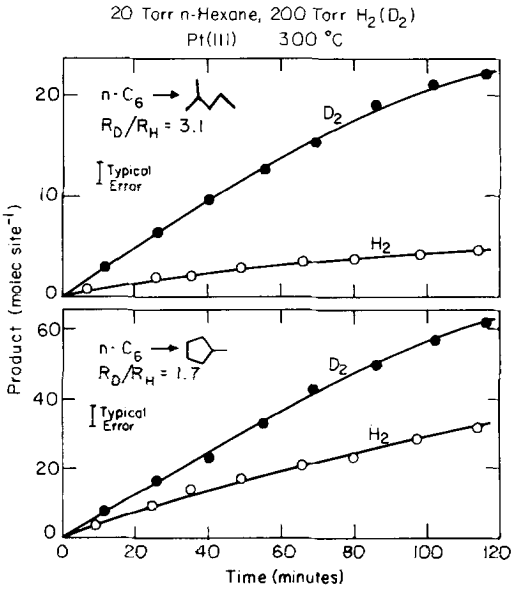

FIG. 1. Comparison between product accumulation curves measured in hydrogen and in deuterium for *n*-hexane isomerization and cyclization catalyzed over Pt(111) at 573 K.

Temperature and Pressure Dependence of the Deuterium Isotope Effects

The temperature dependence of the deuterium isotope effects was investigated

carefully for *n*-hexane reactions catalyzed over the flat (111) and kinked (10,8,7) platinum surfaces. Example Arrhenius plots for these reactions catalyzed in hydrogen and in deuterium are shown in Figs. 2–4. The error bars represent estimated uncertainties that are based on the reproducibility (about ±15%) of the initial rate measurements. Inverse isotope effects for hydrogenolysis and isomerization were exhibited over a wide range of temperature. These isotope effects appeared to decrease in magnitude slightly with increasing temperature. No significant isotope effect was detected for the aromatization reaction over either platinum surface.

Hydrogenolysis and aromatization were the only reactions that displayed "normal" Arrhenius behavior over a wide range of temperature (≈530–650 K). Even for these reactions the apparent activation energies that were in the range of 16–36 kcal/mol appeared to decrease with increasing temperature. The other reactions (isomerization and C_5 cyclization) displayed rate maxima at 570–630 K that have been attributed to a change in composition of the most abundant reaction intermediates as the tem-

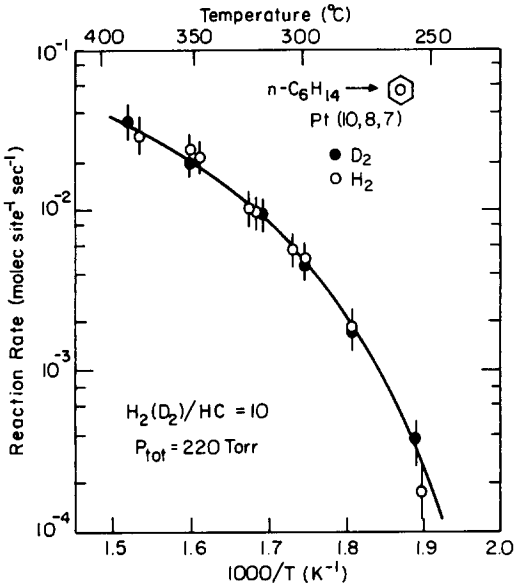

FIG. 3. Arrhenius plot for *n*-hexane aromatization catalyzed in hydrogen and deuterium over the kinked (10,8,7) platinum surface.

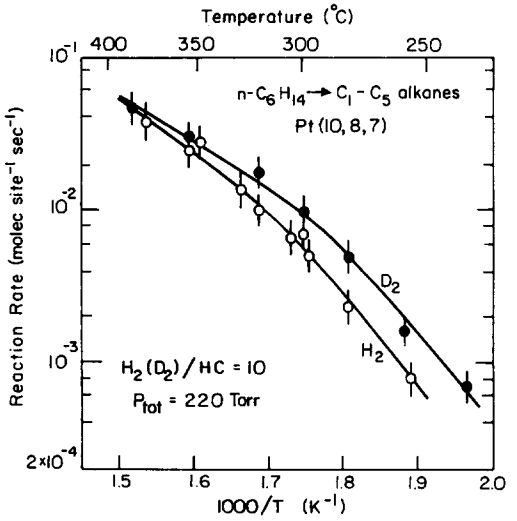

FIG. 2. Arrhenius plots for *n*-hexane hydrogenolysis catalyzed in hydrogen and deuterium over the kinked (10,8,7) platinum surface.

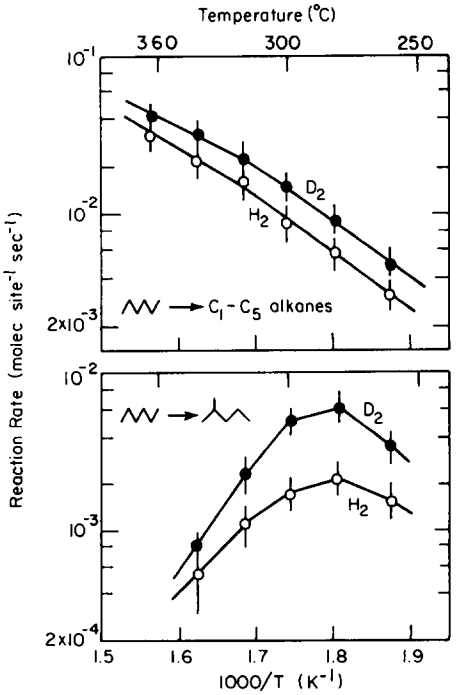

FIG. 4. Arrhenius plots for *n*-hexane hydrogenolysis and isomerization catalyzed over Pt(111).

perature is increased (*8*). Aromatization and hydrogenolysis become favored over isomerization at high temperatures as the intermediate species become more hydrogen deficient. The decreasing activation energies for aromatization and hydrogenolysis at the highest temperatures studied likely arise from a change in reaction mechanism wherein the rate determining step changes from skeletal rearrangement to rehydrogenation or other reaction steps with lower activation energy. More detailed kinetic studies related to this point will be reported separately (*8*).

Initial reaction rates for *n*-hexane hydrogenolysis and aromatization catalyzed at 573 K on the kinked (10,8,7) platinum surface are shown as a function of H_2(or D_2) pressure in Fig. 5. The inverse isotope effect for hydrogenolysis displayed a nearly constant magnitude for all total pressures between 100 and 620 Torr (i.e., R_D/R_H = 1.4–1.8). By contrast, the kinetic isotope effect for aromatization that was negligible at 100–220 Torr increased markedly at higher pressures reaching a value $R_H/R_D \simeq$ 2–3 for total pressures of 620 Torr.

Altered Selectivity for Reactions Catalyzed in Deuterium

Isotope effects measured for the hydrogenolysis and isomerization of isobutane

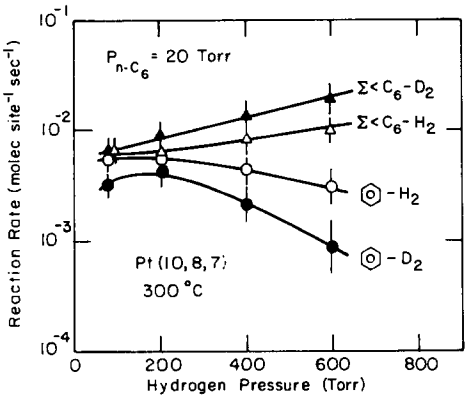

FIG. 5. Comparison between *n*-hexane hydrogenolysis and aromatization rates over Pt(10,8,7) as a function of hydrogen (D_2) pressure.

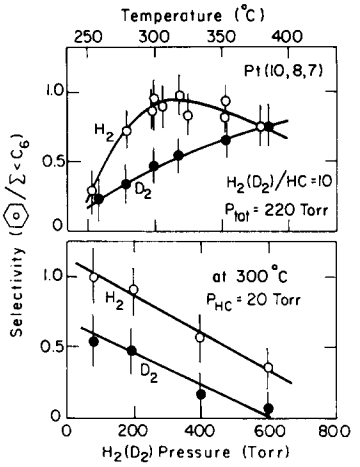

FIG. 6. Initial kinetic selectivities for aromatization over hydrogenolysis determined for *n*-hexane reactions catalyzed in hydrogen and in deuterium over Pt(10,8,7). The selectivities are shown as a function of reaction temperature (upper frame) and hydrogen (D_2) pressure (lower frame).

and neopentane displayed essentially equal magnitudes under all reaction conditions investigated. For these reactions, the selectivity was unaltered by the presence of deuterium. However, with *n*-hexane and *n*-heptane as reactants, parallel reactions generally displayed isotope effects with different magnitudes. In the presence of deuterium, the rate of formation of saturated hydrocarbon products was enhanced relative to the rate of formation of aromatics. As a result, the selectivities for these reactions were altered appreciably. This is shown clearly for *n*-hexane reactions catalyzed on the (10,8,7) platinum surface in Fig. 6, where the kinetic selectivity for aromatization over hydrogenolysis in H_2 and D_2 is shown as a function of reaction temperature and hydrogen (D_2) pressure. The aromatization selectivity in deuterium was reduced over a wide range of reaction conditions. A similar effect was recently noted by Kellner and Bell (*5*) for Fischer–Tropsch reactions catalyzed over silica and alumina supported ruthenium. In that case the kinetic selectivity for C_3- and C_4- olefin synthesis over C_3- and C_4-alkane production was lowered when the reaction rate

studies were carried out in deuterium. Whereas the rates of formation of alkane products displayed inverse isotope effects with magnitudes in the range $R_D/R_H = 1.0$–1.6, the isotope effects for olefin production were always very small, $R_D/R_H \leq 1.2$.

Origin of the Inverse Isotope Effect

An idealized explanation for the inverse isotope effect can be developed using models for hydrogenolysis reaction kinetics proposed by Cimino (*10*), Sinfelt (*11, 12*), Maurel (*13*), and Martin (*14, 15*) and coworkers. Because there exists no proof for these mechanisms or rigorous justification for their extension to skeletal rearrangement reactions catalyzed over platinum crystal surfaces, no attempt will be made here to develop the models in great detail or to distinguish between mechanisms on the basis of isotope effects alone. Further analysis of the isotope effects is discussed elsewhere (*16*).

Previous research by Sinfelt (*12*) and Maurel *et al.* (*13*) revealed that the kinetics of alkane hydrogenolysis catalyzed near atmospheric pressure over platinum can be represented by the reaction sequence

$$H_2 \overset{K_H}{\rightleftharpoons} 2H(ads) \qquad (R1)$$

$$C_nH_{2n+2} \overset{\lambda_H}{\rightleftharpoons} C_nH_x(ads) + \alpha H_2 \qquad (R2)$$

$$C_nH_x(ads) + H_2 \xrightarrow[\text{slow}]{k_H} C_mH_z(ads) + C_{n-m}H_{x-z+2}(ads) \qquad (R3)$$

$$C_mH_z(ads) + C_{n-m}H_{x-z+2}(ads) + H_2 \xrightarrow[\text{fast}]{} \text{products.} \qquad (R4)$$

The key assumption in this scheme is that dissociative chemisorption of both hydrogen and hydrocarbon is rapid and reversible as compared to the rate of hydrogenolysis. Important justification for this assumption under our reaction conditions (530–630 K) was provided by the alkane–deuterium exchange kinetics reported elsewhere (*7*). The rate determining step (R3) presumably involves C–C bond scission in an intermediate species C_nH_x which has lost 2α hydrogen atoms. Detailed studies by Sinfelt (*12*) and Maurel (*13*) revealed that $\alpha = 2$–4 for a wide variety of hydrogenolysis reactions catalyzed near atmospheric pressure over Pt/Al_2O_3. All subsequent reaction steps are assumed to be rapid. Following reasoning discussed previously (*10–13*), this reaction sequence leads to the rate expression

$$R_H = k_H\lambda_H P_C P_{H_2}/(K_H{}^{\alpha}P_{H_2}{}^{\alpha} + \lambda_H P_C) \qquad (1)$$

where K_H, λ_H, and k_H are equilibrium constants and rate constants defined by the reactions (R1)–(R3), and P_C and P_{H_2} are the partial pressures of hydrocarbon and hydrogen, respectively. Regardless of the exact form of the rate determining step, this rate expression indicates that apparent reaction rates involve a complex product of elementary rate coefficients and adsorption equilibrium constants. The measured isotope effects therefore appear to arise from a combination of kinetic and thermodynamic isotope effects. A similar conclusion was reached by Kellner and Bell in recent studies of Fischer–Tropsch reactions catalyzed over supported ruthenium catalysts (*5*).

Using Eq. (1), the inverse isotope effect should have a magnitude given by

$$\frac{R_D}{R_H} = \sum_{i=0}^{2(\beta-\alpha)} \frac{\gamma_i k_{Di}\lambda_{Di}}{(K_D{}^{\alpha}P_{D_2}{}^{\alpha} + \lambda_{Di}P_C)} \Big/ \frac{k_H\lambda_H}{(K_H{}^{\alpha}P_{H_2}{}^{\alpha} + \lambda_H P_C)} \qquad (2)$$

where γ_i is the fraction of surface intermediate species in the presence of deuterium that contain i hydrogen atoms, and K_D, λ_{Di}, and k_{Di} are constants defined by the reactions

$$D_2 \overset{K_D}{\rightleftharpoons} 2D(ads) \qquad (R5)$$

$$C_nH_{2n+2} + \left(\beta - \frac{i}{2}\right)D_2 \overset{\lambda_{Di}}{\rightleftharpoons} C_nH_iD_{x-i}(ads) + \alpha D_2 + \left(\beta - \frac{i}{2}\right)H_2 \qquad (R6)$$

$$C_nH_iD_{x-i}(ads) + D_2 \xrightarrow{k_{Di}} C_mH_jD_z(ads) + C_{n-m}H_{i-j}D_{x+2-i-z}(ads). \qquad (R7)$$

The sum over $i = 0, 1, 2, \ldots, 2(\beta - \alpha)$ where $\beta = n + 1 = \alpha + x/2$ includes a distribution of intermediates with variable deuterium and constant hydrogen plus deuterium contents. In the limiting case where complete exchange takes place before skeletal rearrangement $i = 0$, $\gamma_0 = 1$, and Eq. (2) simplifies to

$$\frac{R_D}{R_H} = \frac{k_D\lambda_D(K_H{}^{\alpha}P_{H_2}{}^{\alpha} + \lambda_H P_C)}{k_H\lambda_H(K_D{}^{\alpha}P_{D_2}{}^{\alpha} + \lambda_D P_C)}. \quad (3)$$

This situation appears to be realistic under our reaction conditions as indicated by the facts that (1) complete deuterium exchange was typically 100 times faster than skeletal rearrangement (*7*), and (2) all reaction products appeared to be extensively if not completely deuterated. While it is highly unlikely that complete exchange prevails for *every* reacting molecule, application of this useful assumption permits a separation of the kinetic and thermodynamic isotope effects and a qualitative evaluation of the latter's importance.

The factor K_D/K_H appearing in Eq. (3) can be evaluated directly using statistical considerations together with Pt–H (Pt–D) stretching frequencies recently reported by Primet (*17*) and Ibach *et al.* (*18, 19*) that are summarized in Table 2 for the two cases of weak "reversible" and strong "irreversible" hydrogen chemisorption. Reversibly adsorbed hydrogen displays a single stretching frequency of 2120 cm^{-1} (*17*) and can be modeled as a mobile two-dimensional gas. In this case,

$$\frac{K_D}{K_H} = \left(\frac{M_{H_2}}{M_{D_2}}\right)^{1/2}\left(\frac{1 - \exp(-h\nu_{M-H}/kT)}{1 - \exp(-h\nu_{M-D}/kT)}\right)^2 \left(\frac{1 - \exp(-h\nu_{D_2}/kT}{1 - \exp(-h\nu_{H_2}/kT)}\right) \times \exp\{[2(\nu_{M-H} - \nu_{M-D}) - (\nu_{H_2} - \nu_{D_2})]n/2kT\} \quad (4)$$

where M_{H_2} and M_{D_2} are molecular masses of H_2 and D_2 and ν_{M-H} and ν_{M-D} are vibrational frequencies given in Table 2. This function predicts that K_D/K_H should increase slowly with increasing temperature from 0.54 to 0.64 for temperatures between 273 and 673 K. Strongly chemisorbed hydrogen displays two stretching frequencies (ν_A = 550 cm^{-1}, ν_E = 1230 cm^{-1}). Since in this case, the hydrogen and deuterium atoms are immobile with 3 degrees of vibrational freedom, K_D/K_H can be estimated using

$$\frac{K_D}{K_H} = \left(\frac{M_{H_2}}{M_{D_2}}\right)^{5/2}\left(\frac{1 - \exp(-h\nu_A{}^H/kT)}{1 - \exp(-h\nu_A{}^D/kT)}\right)^2 \left(\frac{1 - \exp(-h\nu_E{}^H/kT)}{1 - \exp(-h\nu_E{}^D/kT)}\right)^4 \left(\frac{1 - \exp(-h\nu_{D_2}/kT)}{1 - \exp(-h\nu_{H_2}/kT)}\right) \times \exp\{[2(\nu_A{}^H + 2\nu_E{}^H - \nu_A{}^D - 2\nu_E{}^D) - (\nu_{H_2} - \nu_{D_2})]/h/2kT\}. \quad (5)$$

This function varies from 0.70 at 273 K to 0.58 at 673 K and displays a minimum of 0.55 at about 470 K. It appears clear that $K_D/K_H \simeq 0.6$ for both types of surface hydrogen under reaction conditions appropriate to the work described here.

It should be noted that for the strongly chemisorbed hydrogen species Eq. (5) predicts that the heat of deuterium chemisorption on platinum should exceed that for hydrogen by about 0.7 kcal/mole. Little or no difference is predicted for the weaker reversible chemisorption. The former prediction is in close accord with the experimen-

TABLE 2

Stretching Frequencies for Molecular and Chemisorbed Hydrogen and Deuterium (*17–19*)

Species	Mode	Frequency (cm^{-1})
H_2	$\nu_{A_1} = \nu_{H_2}$	4160
D_2	$\nu_{A_1} = \nu_{D_2}$	2990
Pt–H[a]	$\nu_A = \nu_A{}^H$	550
	$\nu_E = \nu_E{}^H$	1230
Pt–D[a]	$\nu_A = \nu_A{}^D$	400
	$\nu_E = \nu_E{}^D$	900
Pt–H[b]	$\nu_A = \nu_{M-H}$	2120
Pt–D[b]	$\nu_A = \nu_{M-D}$	1585

[a] Immobile, "irreversible" chemisorption.
[b] Mobile, "reversible" chemisorption.

tal results of Gundry (*20*) and Wedler *et al.* (*21*) which indicate that deuterium is more strongly chemisorbed on nickel as compared to hydrogen by 0.6–1.0 kcal/mole. Gundry (*20*) also noted that K_D/K_H decreased with increasing temperature from about 2.4 near 180 K to unity at 270 K. At higher temperatures of catalytic importance, the contribution of zero point energy differences to K_D/K_H in Eq. (5) becomes small compared with the contribution of the preexponential factor so that the magnitude of K_D/K_H is less than unity. Creative experiments are needed to clarify which if either of these hydrogen species is actually important in the reaction pathway leading to alkane hydrogenolysis.

The ratio of hydrocarbon adsorption equilibrium constants λ_D/λ_H defined by reactions (R2) and (R6) (with $i = 0$) can be expressed by

$$\frac{\lambda_D}{\lambda_H} = \left(\frac{Q_{H_2}}{Q_{D_2}}\right)^{\beta-\alpha} \frac{Q_{CD_x}}{Q_{CH_x}} \qquad (6)$$

where the Q_i are the total partition functions for the reacting species. If it is assumed that the intermediate species are immobile it follows that

$$\frac{\lambda_D}{\lambda_H} = \left[\left(\frac{M_{H_2}}{M_{D_2}}\right)^{5/2}\left(\frac{1-\exp(-h\nu_{D_2}/kT)}{1-\exp(-h\nu_{H_2}/kT)}\right)\right]^{(\beta-\alpha)} \Pi_g\left(\frac{1-\exp(-h\nu_g^{CH_x}/kT)}{1-\exp(-h\nu_g^{CD_x}/kT)}\right) \times \exp\{[(\nu_{D_2}-\nu_{H_2})(\beta-\alpha)h - 2(E_{CD_x}{}^0 - E_{CH_x}{}^0)]/2kT\} \qquad (7)$$

where $\nu_g^{CH_x}$ and $\nu_g^{CD_x}$ are normal modes for the intermediate C_nH_x (C_nD_x) species and $E_{CD_x}{}^0 - E_{CH_x}{}^0$ is the difference in zero point energies between deuterated and hydrogenated intermediates. According to Ozaki (*1*), this zero point energy difference corresponds to approximately 1.8 kcal/mole per C–H (C–D) bond. Table 3 summarizes λ_D/λ_H ratios calculated for several alkanes at 273 and 573 K using Eq. (7) with α varied between one and four. The magnitude of the vibrational partition function has been estimated for a chain of $x/2$ CH_2 (CD_2) groups with local symmetry C_{2v} (*22*). At low temperatures the model calculations produce the result that $\lambda_D/\lambda_H \gg 1$, whereas at 573 K λ_D/λ_H is on the order of 2–5 independent of α and the nature of the reacting hydrocarbon. When exact partition functions for C_nH_x and C_nD_x are included, the λ_D/λ_H ratios may become larger, but by no more than about a factor of 2 at most. While the contribution of the zero point energy difference to the thermodynamic isotope effect clearly diminishes markedly with increasing temperature, it is important to note that this effect on the surface concentration of hydrocarbon intermediates is always predicted to contribute to the inverse isotope effect.

Detailed information concerning the configuration and vibrational frequencies of the activated complexes is needed to obtain a meaningful estimate for the magnitude of k_D/k_H. While little zero point energy difference (and kinetic isotope effect) would be

TABLE 3

Temperature Dependence of the Hydrocarbon Adsorption Equilibrium Constant Ratio λ_D/λ_H

Hydrocarbon	α	$(\beta - \alpha)$	$E_{CH_x}{}^0 - E_{CD_x}{}^0$ [a]	λ_D/λ_H	
			(kcal/mole)	298 K	573 K
C_4H_{10}	3	2	7.2	41	1.6
C_5H_{12}	3	3	10.8	302	2.3
C_6H_{14}	1	6	21.6	8.7×10^4	5.2
C_6H_{14}	2	5	18.0	1.4×10^4	4.0
C_6H_{14}	3	4	14.4	2.0×10^3	3.0

[a] $E_{CH_x}{}^0 - E_{CD_x}{}^0 \approx 1.8x$ (kcal/mole), Ref. (*1*).

expected for unimolecular C–C bond breaking or skeletal rearrangement, the rate determining step presumably involves a hydrogenation process where the zero point energy difference is substantial. For hydrogenation reactions it is usually observed that $k_H \geq k_D$ (*1*).

It has been assumed in this analysis that no competition exists between deuterium (H_2) and hydrocarbon for platinum surface sites. According to the "landing site" models for hydrocarbon–deuterium exchange (*23*) and ethane or propane hydrogenolysis (*14, 15*), reaction rates are controlled by the rate of irreversible hydrocarbon chemisorption and dehydrogenation on surface sites that contain at least Z adjacent metal atoms that are free from chemisorbed hydrogen (deuterium). Rate expressions of the form

$$R = kP_C(1 - \theta_H)^Z \qquad (8)$$

are predicted by these competitive models where $(1 - \theta_H)^Z$ is the probability of having a ensemble of Z uncovered atoms. In this case, the deuterium isotope effects should have magnitudes given by

$$R_D/R_H \simeq k_D(1 - \theta_D)^Z/k_H(1 - \theta_H)^Z. \qquad (9)$$

From previous consideration of K_H and K_D we expect that $\theta_D < \theta_H$. Since Z reportedly assumes values of 10–15 (*14, 15*), it appears that kinetic models which allow for competitive chemisorption of the reactants also lead to the prediction that inverse isotope effects should exist for hydrocarbon reactions catalyzed in the presence of deuterium gas.

As compared to the other *n*-hexane skeletal rearrangement reactions, aromatization displayed unique behavior characterized by a normal kinetic isotope effect. Parallel reactions are expected to display isotope effects with different magnitudes depending upon the site requirements and the deuterium content of the reaction intermediates. According to Eqs. (2), (7), and (9), R_D/R_H should decrease with decreasing ensemble size and decreasing deuterium content. Since aromatization selectivities are maximized at high reaction temperatures (*8*), it is likely that the reaction intermediates leading to benzene production have lower hydrogen plus deuterium content than those leading to the other skeletal rearrangement reactions. This difference in hydrogen content could account in part for the altered selectivities for reactions catalyzed in deuterium. Differences in site requirements or k_D/k_H might also contribute to the altered aromatization selectivity. More detailed studies using other types of catalysts would be valuable to differentiate between these possibilities.

ACKNOWLEDGMENT

This work was supported by the Director, Office of Energy Research, Office of Basic Energy Sciences, Materials Sciences Division of the U.S. Department of Energy under Contract W-7405-ENG-48.

REFERENCES

1. Ozaki, A., "Isotopic Studies of Heterogeneous Catalysis," Academic Press, New York, 1977.
2. Knozinger, H., and Scheglita, A., *J. Catal.* **17,** 252 (1970).
3. Inoue, Y., and Yasumori, I., *J. Phys. Chem.* **75,** 880 (1971).
4. Wilson, T. P., *J. Catal.* **60,** 167 (1979).
5. Kellner, S., and Bell, A., *J. Catal.* **67,** 175 (1981).
6. Aika, K., and Ozaki, A., *J. Catal.* **14,** 311 (1969); **19,** 350 (1970).
7. Davis, S. M., and Somorjai, G. A., *J. Phys. Chem.*, in press.
8. Davis, S. M., Zaera, F., and Somorjai, G. A., *J. Catal.*, in press.
9. Gas chromatographic resolution of isotopic molecules appears to arise from a combination of effects including thermodynamic isotope effects on adsorption–desorption, and differences in rotational entropy. For further discussion see S. Akhter and H. A. Smith, *Chem. Rev.* **64,** 261 (1964), and R. Yaris and J. R. Sams, *J. Chem. Phys.* **37,** 571 (1962).
10. Cimino, A., Boudart, M., and Taylor, H. S., *J. Phys. Chem.* **58,** 796 (1954).
11. Sinfelt, J. H., *in* "Advances in Catalysis," Vol. 23, p. 91, Academic Press, New York, 1973.
12. Sinfelt, J. H., and Taylor, W. F., *J. Chem. Soc. Faraday Trans.* **64,** 3086 (1968).
13. Leclercq, G., Leclercq, L., and Maurel, R., *J. Catal.* **44,** 68 (1976).

14. Martin, G. A., *J. Catal.* **60,** 345 (1979).
15. Dalmon, J. A., and Martin, G. A., *J. Catal.* **66,** 214 (1980).
16. Davis, S. M., Ph.D. thesis, University of California, Berkeley, 1981.
17. Candy, J. P., Fauilloux, F., and Primet, M., *Surf. Sci.* **72,** 167 (1978).
18. Baro, A. M., and Ibach, H., *Surf. Sci.* **92,** 237 (1980).
19. Baro, A. M., Bruchman, H. D., and Ibach, H., *Surf. Sci.* **88,** 384 (1979).
20. Gundry, P. M., "Proceedings, 2nd International Congress on Catalysis," Paper 51, Paris, 1960.
21. Wedler, G., Broker, F. J., Fisch, G., and Schroll, G., *Z. Phys. Chem. N.F.* **76,** 212 (1971).
22. The CH_2 (CD_2) frequencies used for this calculation were $\upsilon_{A_1} = 2940\ cm^{-1}$ ($2150\ cm^{-1}$), $\upsilon_{B_2} = 2850\ cm^{-1}$ ($2080\ cm^{-1}$), $\upsilon_{A_1} = 1450\ cm^{-1}$ ($1060\ cm^{-1}$), $\upsilon_{B_1} = 1350\ cm^{-1}$ ($990\ cm^{-1}$), $\upsilon_{A_2} = 1200\ cm^{-1}$ ($880\ cm^{-1}$), and $\upsilon_{B_2} = 730\ cm^{-1}$ ($530\ cm^{-1}$).
23. Frennet, A., Lienard, G., Crucq, F., and Delgols, L., *J. Catal.* **53,** 150 (1978); **35,** 18 (1974).